



HAL
open science

Nanopatterning the electronic properties of gold surfaces with self-organized superlattices of metallic nanostructures

Clement Didiot, Stéphane Pons, Bertrand Kierren, Yannick Fagot-Revurat,
Daniel Malterre

► To cite this version:

Clement Didiot, Stéphane Pons, Bertrand Kierren, Yannick Fagot-Revurat, Daniel Malterre. Nanopatterning the electronic properties of gold surfaces with self-organized superlattices of metallic nanostructures. *Nature Nanotechnology*, 2007, 2 (10), pp.617-621. 10.1038/nnano.2007.301 . hal-04434757

HAL Id: hal-04434757

<https://hal.science/hal-04434757>

Submitted on 2 Feb 2024

HAL is a multi-disciplinary open access archive for the deposit and dissemination of scientific research documents, whether they are published or not. The documents may come from teaching and research institutions in France or abroad, or from public or private research centers.

L'archive ouverte pluridisciplinaire **HAL**, est destinée au dépôt et à la diffusion de documents scientifiques de niveau recherche, publiés ou non, émanant des établissements d'enseignement et de recherche français ou étrangers, des laboratoires publics ou privés.

Nanopatterning the electronic properties of gold surfaces with self-organised superlattices of metallic nanostructures

Clément Didiot, Stéphane Pons,^{*} Bertrand Kierren, Yannick Fagot-Revurat and Daniel Malterre

Laboratoire de Physique des Matériaux UMR7556, Nancy-Université - CNRS, Boîte

Postale 239, F-54506 Vandoeuvre-lès-Nancy, France

^{*} corresponding author: stephane.pons@lpm.u-nancy.fr

The self-organised growth of nanostructures on surfaces could offer many advantages in the development of new catalysts, electronic devices and magnetic data-storage media [1–5]. The local density of electronic states on the surface at the relevant energy scale strongly influences chemical reactivity[6–9], as does the shape of the nanoparticles[10]. The electronic properties of surfaces also influence the growth and decay of nanostructures such as dimers, chains and superlattices of atoms or noble metal islands[9, 36, 11–15]. Furthermore, controlling these properties on length scales shorter than the diffusion lengths of the electrons and spins (some 10s of nm for metals) is a major goal in electronics and spintronics[16]. However, to date there have been few reports on the electronic properties of self-organised nanostructures[17–19]. Here we report the self-organised growth of macroscopic superlattices of Ag or Cu nanostructures on Au vicinal surfaces, and demonstrate that the electronic properties of these systems depend on the balance between the confinement and the perturbation of the surface states caused by the steps and the nanostructures superlattice. We also show that the local density of states can be modified in a controlled way by adjusting simple parameters such as the metal deposited and the degree of coverage.

Vicinal surfaces are produced by cutting a surface at a small angle with respect to a high symmetry plane to create a surface that consists of flat terraces separated by atomic step edges. The repulsion between the step edges can induce a regular spacing of the steps. The index of the vicinal surface (Miller indices) is directly linked to the orientation of the terrace and to the miscut

angle, then to the size of the terraces. Au(788) and Au(23 21 21) are stable vicinal surfaces exhibiting an array of homogenous terraces oriented in the (111) direction. The terraces in both Au(788) and Au(23 23 21) are separated by 111-like steps. Recent work has shown that the steps introduce a periodic potential that confines or perturbs the Shockley state of these surfaces. Shockley states are sp-surface states showing behaviour of bidimensional (2D) free electrons on flat surfaces – i.e. parabolic band structures. In vicinal surfaces, the resulting modification of the band structure depends on the terrace size[20–22]. Au(23 23 21) has large terraces with an average width $d=57\pm 5\text{\AA}$ and there is good confinement of the surface states in the terraces. Au(788) has smaller ($d=38\pm 4\text{\AA}$) terraces and the surface states interact more with the bulk states, so they are less confined to the surface and more delocalized throughout the crystal.

The terraces of Au(111) vicinal surfaces exhibit a surface reconstruction derived from the extensively studied chevron reconstruction[23] of Au(111). Stacking fault lines that are perpendicular to the steps periodically separate fcc and hcp domains (fig 1a). The periodicities of the reconstruction are $l=72\pm 4\text{\AA}$ for Au(788) and $l=66\pm 4\text{\AA}$ for Au(23 23 21). We have recently shown that the reconstruction modifies the electronic properties of the surface and that several gaps open in the surface band structure of Au vicinal surfaces[24].

As a result, the electronic properties of vicinal surfaces are perturbed in two directions - perpendicular and parallel to the step edges – and this leads to a periodic modulation of the local density of electronic states (LDOS). Previous experiments have shown that modulations of the LDOS associated with confined or perturbed surface states on clean surfaces[25–27] and heteroepitaxial systems[28] can be observed with scanning tunnelling spectroscopy (STS) as standing waves patterns in conductance (dI/dV) images. The perfect structural order displayed by Au(788) is reflected in the periodic LDOS pattern seen in the conductance images at different energies (fig 1b,c,d). There is an ongoing debate on the nature (one-dimensional (1D) versus 2D) of the surface state electron gas on vicinal surfaces. Up to now, no consideration of the localisation of the electronic density was clearly addressed for the comparison between 1D and 2D behaviour in perfect vicinal systems. In the energy range of dI/dV images of fig. 1, the data are compatible with a strong confinement (1D) model or a periodic perturbation (2D) model of the surface states by the step edges.

Vicinal surfaces are known to present an array of nucleation sites for various transition metal adatoms provided that their interactions with hcp, fcc and faulted sites are different. In the case of silver adatoms on a gold surface, we found out that the growth process differs from previously reported systems[5]. Atomic exchanges are not observed at the step edges or on top of the terraces, and only one adsorption site per unit cell of the reconstructed substrate is involved. As shown in fig. 2a, for this coverage and over a small range of deposition temperatures – 80K to ~150K - each fcc domain of Au(788) is occupied by one (111)-oriented island. The normalised distribution of nearest neighbour distances in the direction parallel to the step is monodisperse with a HWHM of 0.13 (fig. 2b). Since the nanostructures are connected to the step edges, the perpendicular distance is given by the terrace width.

For deposition between 120K and 135K, the size distribution of the nanostructures is very sharp (fig. 2c). Moreover, as illustrated in fig. 2a, the triangular shapes of the islands are highly homogeneous. This happens because the temperature is low enough to allow self-organized growth (with the Ag adatoms being trapped in fcc domains) during deposition but, at the same time, prevent dendritic growth[29]. We assume that the early stages of growth are driven by the stress due to the reconstruction, the lattice of steps and, possibly, by the LDOS pattern of the clean surface. Thus, for temperatures between 120K and 135K, the average size of the islands and the distance between two nanostructures are definitely controlled by the vicinality of the surface - which also drives the reconstruction patterns[30] - and by the Ag coverage. Statistical considerations of nucleation[3] in a network of uniform identical traps would lead to a theoretical standard deviation of $\sigma^{1D}_u \approx 0.05$ for parameters of figure 2a. A Gaussian fit of the nanostructures size leads to a HWHM of 0.15. This value indicates that the main broadening of the dispersion curves is related to the natural dispersion of the terrace and reconstruction sizes. A unit cell of $S \approx 27.4 \pm 4.4 \text{ nm}^2$ can be defined for the Au(788) clean surface as shown in fig. 1a. As a result, a estimated value of $\sigma^{1D}_e \approx 0.13$ – very close to the experimental data - is obtained by taking into account the convolution with the size distribution of the unit cell of the substrate $\Delta S/S$ and σ^{1D}_u .

Ag films on Au(111) are known to exhibit a Shockley state[31], so electronic properties of the surface reflect its structural periodicity. We show in fig. 2d and 2e that the self-organised system

exhibits standing waves which are homogenous at large scale and become more and more complex as the energy increases. An analysis of the LDOS patterns at different locations on the sample shows a complete homogeneity of the electronic properties at the macroscopic scale whose standing wave patterns do not change and consist in a repetition of a unit cell. Finally, the global pattern remains undisturbed by the limited local disorder.

At low energy, the electronic properties are similar to those of the clean surface: the LDOS is mostly localised in hcp domains (fig. 3b). As the energy increases the LDOS maxima shift in the uncovered fcc domain parts (fig. 3c). Ag islands are still unoccupied by the surface states even at intermediate energy (fig. 3d), which means that Ag acts as a weak repulsive potential. Nevertheless, the Shockley state can overcome this potential at sufficiently high energy and standing waves patterns are observed in Ag islands at $E = -0.065\text{eV}$ (fig 3e). Thus, in contrast with the bare vicinal surface, the Ag-Au sample exhibits a substantial enhancement of the LDOS close to the Fermi energy, E_F , at the Ag nanostructures. The potential associated with the step edges is quite strong because no maxima of the LDOS are localised on the edges for these energies. A careful analysis of the electronic properties of samples with a different coverage and/or a vicinal index gives the same tendencies as presented in fig. 3 even if the energy ranges associated to each standing wave pattern may be different. The colour scale of fig. 3b-e reflects the variation of the LDOS (which is caused by quantum interference between the electrons) with respect to the spatial average contribution of the Shockley state to the LDOS. Since the islands are connected to the terraces, the understanding of the LDOS patterns cannot be based on the simple analysis of triangular quantum boxes[32]: the whole system must be considered as a 2D coherent electron gas described by scattered Bloch waves in a 2D periodic potential. A schematic view of this potential is shown in fig. 3f.

In the following we show that the 2D potential can be modified by selecting different vicinal indexes, deposited materials or coverage. For example, when Cu is deposited on Au(23 23 21), it self-organises to form lattices of bilayer islands at step edges in fcc domains (fig. 4a). Although the quality of the lattice and the homogeneity of the Cu nanostructures sizes do not match those observed in Ag superlattices, the Cu dots still exert a strong repulsive potential for the surface states (fig. 4f). Indeed the interfacial barrier is stronger than for Ag because of the bilayer height

of the islands. Therefore, Cu nanostructures correspond to isolated dots, i.e. the electronic states of the islands do not couple to the ones of the surrounding gold terrace. Moreover, no standing waves develop in the Cu islands until 300meV above E_F due to their reduced size as seen in fig. 4e. The symmetry of the Cu-Au system is rectangular rather than triangular like the Ag-Au system due to the compact shape of the nanostructures. As a result, the LDOS in the uncovered Au surface is quadratic (fig. 4b-d). Figure 4g compares STS spectra recorded at the centre of Ag or Cu nanostructures, with the peaks corresponding to the onset energy of the surface states (as in fig. 3e). These spectra show that the onset energy for Ag nanostructures decreases as they increase in size, as is expected for a confined or perturbed system. For Cu nanostructures, on the other hand, the onset energy is shifted far above E_F , unlike the Ag/Au(23 23 21) system, where the onset energy is close to that for a clean gold surface, and the Ag/Au(788) system, where the onset energy is close to E_F (fig. 3e).

We have shown that we can modify the electronic properties of surfaces at the nanoscale over a large range of energies by making a self-organised array of Ag or Cu nanostructures on gold vicinal surfaces. Ag deposition leads to the formation of a superlattice of monodisperse triangular nanostructures. Moreover, depending on very simple parameters such as the nature of the deposited compound (Ag or Cu), the index of the vicinal surface and the coverage, it is possible to modify the electronic properties of the surface. One possible outlook of this work is to replace noble metal nanostructures by molecular complexes[33] or transition metals because the electronic and magnetic properties of these deposited materials may influence the behaviour of the surface states. It might also be possible to pattern the LDOS of the bulk states at the nanoscale. Finally, although the chemical properties of these systems have yet to be characterized, these self-organised systems, exhibiting some 10^{13} nanostructures per square inch, could be used as templates for growing single atom or molecular lattices, bimetallic nanostructures or supramolecular hybrid systems[34].

METHODS

We used a scanning tunnelling microscope working at 5K combined to a multi-chamber setup under ultra-high vacuum described elsewhere[31]. Au(788) and Au(23 23 21) were prepared by cycles of Ar^+ sputtering and annealing at 800K. We paid special attention to the preparation of

the vicinal surface in order to be sure that the highly reactive specific adsorption sites for Ag atoms were free from defects before deposition. Four temperature steps of a few minutes (750K to 400K) were used during the cooling of the sample after annealing. This method produces a well ordered stepped surface exhibiting a reconstruction pattern with a minimum amount of defects which are known to have a dramatic influence on surface bands. The ability of this procedure to produce perfectly clean surfaces has been established using angle resolved photoemission spectroscopy measurements prior to this study[24]. Low deposition rates of Ag and Cu (<1ML/min) were achieved from Knudsen cells. Ag and Cu were evaporated onto the substrate cooled at 130K and the temperature of the sample was kept under 150K during the transfer to the 5K STM stage. A ML refers to a mono-atomic covering of the surface.

Bias voltages indicated for STM and STS data correspond to sample potentials with respect to the grounded tip. A modulation of 10mV rms at 700Hz was added to the sample bias for lock-in assisted STS measurements. The colour scale of fig. 3 was calculated as follows: firstly, the (x,y) spatial average of the conductance spectra $\langle dI(E)/dV \rangle$ was evaluated. Secondly, the average contribution from the surface states, $\langle dI(E)/dV \rangle_{ss}$, was extracted from $\langle dI(E)/dV \rangle$ by subtracting a background level associated to bulk states, using the method given in reference[35]. Finally, the contrast of the conductance images $dI(E,x,y)/dV$ refers to the comparison of the LDOS modulations with $\langle dI(E)/dV \rangle_{ss}$.

ACKNOWLEDGEMENTS

The authors would like to thank Luc Moreau for his technical support.

AUTHOR CONTRIBUTIONS

C. D. and S. P. performed the experiments. C. D., S. P. and B. K. analyzed the data. S. P. wrote the resulting paper. All the authors discussed the results and commented on the manuscript. Please write to S. P. for commentary, discussion or suggestions.

REFERENCES

- [1] Barth, J. V., Costantini, G. & Kern, K. Engineering atomic and molecular nanostructures at surfaces. *Nature* **437**, 671-679 (2005).
- [2] Rosei, F. Nanostructured surfaces: challenges and frontiers in nanotechnology. *J. Phys. Condens. Matter* **16**, S1373–S1436 (2004).
- [3] Brune, H., Giovannini, M., Bromann, K. & Kern, K. Self-organised growth of nanostructure arrays on strain-relief patterns. *Nature* **394**, 451–453 (1998).
- [4] Gambardella, P. *et al.* Ferromagnetism in one-dimensional monatomic metal chains. *Nature* **416**, 301–304 (2002).
- [5] Repain, V., Berroir, J. M., Rousset, S. & Lecoer, J. Growth of self-organised cobalt nanostructures on Au(111) vicinal surfaces. *Surf. Sci.* **447**, L152–L156 (2000).
- [6] Hoffmann, R. A chemical and theoretical way to look at bonding on surfaces. *Rev. Mod. Phys.* **60**, 601–628 (1988).
- [7] Valden, M., Lai, X. & Goodman, D. W. Onset of catalytic activity of gold clusters on titania with the appearance of nonmetallic properties. *Science* **281**, 1647–1650 (1998).
- [8] Aballe, L., Barinov, A., Locatelli, A., Heun, S. & Kiskinova, M. Tuning surface reactivity via electron quantum confinement. *Phys. Rev. Lett.* **93**, 196103 (2004).
- [9] Lau, K. H. & Kohn, W. Indirect long-range oscillatory interaction between adsorbed atoms. *Surf. Sci.* **75**, 69–85 (1978).
- [10] Lopez, N. & Nørskov, J. K. Catalytic CO oxidation by a gold nanoparticle: A density functional study. *J. Am. Chem. Soc.* **124**, 11262–11263 (2002).
- [11] Morgenstern, K., Braun, K.-F. & Rieder, K.-H. Direct imaging of Cu dimer formation, motion, and interaction with Cu atoms on Ag(111). *Phys. Rev. Lett.* **93**, 56102 (2004).
- [12] Silly, F. *et al.* Creation of an atomic superlattice by immersing metallic adatoms in a two-dimensional electron sea. *Phys. Rev. Lett.* **92**, 16101 (2004).
- [13] Memmel, N. & Bertel, E. Role of surface states for the epitaxial growth on metal surfaces. *Phys. Rev. Lett.* **75**, 485–488 (1995).
- [14] Fichthorn, K. A. & Merrick, M. L. Nanostructures at surfaces from substrate-mediated interactions. *Phys. Rev. B* **68**, 41404 (2003).
- [15] Morgenstern, K., Lægsgaard, E. & Besenbacher, F. Quantum size effects in adatom island decay. *Phys. Rev. Lett.* **94**, 166104 (2005).

- [16] Manoharan, H. C., Lutz, C. P. & Eigler, D. M. Tunneling into a single magnetic atom: Spectroscopic evidence of the Kondo resonance. *Nature* **403**, 512–515 (2000).
- [17] Losio, R. *et al.* Band splitting for Si(557)-Au: Is it spin-charge separation? *Phys. Rev. Lett.* **86**, 4632–4635 (2001).
- [18] Ternes, M. *et al.* Scanning-tunneling spectroscopy of surface-state electrons scattered by a slightly disordered two-dimensional dilute solid: Ce on Ag(111). *Phys. Rev. Lett.* **93**, 146805 (2004).
- [19] Schiller, F., Ruiz-Osés, M., Cordón, J. & Ortega, J. Scattering of surface states at step edges in nanostripe arrays. *Phys. Rev. Lett.* **95**, 66805 (2005).
- [20] Ortega, J. E. *et al.* One-dimensional versus two-dimensional surface states on stepped Cu(111). *Phys. Rev. B* **65**, 165413 (2002).
- [21] Mugarza, A. & Ortega, J. E. Electronic states at vicinal surfaces. *J. Phys. Cond. Mat.* **15**, S3281–S3310 (2003).
- [22] Baumberger, F. *et al.* Step-lattice-induced band-gap opening at the Fermi level. *Phys. Rev. Lett.* **92**, 16803 (2004).
- [23] Barth, J. V., Brune, H., Ertl, G. & Behm, R. J. Scanning tunneling microscopy observations on the reconstructed Au(111) surface: Atomic structure, long-range superstructure, rotational domains, and surface defects. *Phys. Rev. B* **42**, 9307–9318 (1990).
- [24] Didiot, C. *et al.* Reconstruction-induced multiple gaps in the weak coupling limit: The surface bands of Au(111) vicinal surfaces. *Phys. Rev. B* **74**, R81404 (2006).
- [25] Hasegawa, Y. & Avouris, P. Direct observation of standing wave formation at surface steps using scanning tunneling spectroscopy. *Phys. Rev. Lett.* **71**, 1071–1074 (1993).
- [26] Li, J., Schneider, W. D., Berndt, R. & Crampin, S. Electron confinement to nanoscale Ag islands on Ag(111): A quantitative study. *Phys. Rev. Lett.* **80**, 3332–3335 (1998).
- [27] Chen, W., Madhavan, V., Jamneala, T. & Crommie, M.F. Scanning tunneling microscopy observation of an electronic superlattice at the surface of clean gold. *Phys. Rev. Lett.* **80**, 1469–1472 (1998).
- [28] Pons, S., Mallet, P. & Veuille, J.-Y. Electron confinement in nickel and copper nanostructures on Cu(111). *Phys. Rev. B* **64**, 193408 (2001).
- [29] Ovesson, S., Bogicevic, A. & Lundqvist, B. I. Origin of compact triangular islands in metal-on-metal growth. *Phys. Rev. Lett.* **83**, 2608–2611 (1999).

[30] Rousset, S., Repain, V., Baudot, G., Garreau, Y. & Lecoeur, J. Self-ordering of Au(111) vicinal surfaces and application to nanostructure organised growth. *J. Phys.: Condens. Matter* **15**, S3363–S3392 (2003).

[31] Cercellier, H. *et al.* Interplay between structural, chemical and spectroscopic properties of Ag/Au(111) epitaxial ultrathin films: A way to tune the rashba coupling. *Phys. Rev. B* **73**, 195413 (2006).

[32] Pons, S., Mallet, P., Magaud, L. & Veillen, J.-Y. Investigation of the Ni(111) Shockley-like surface state using confinement to artificial nanostructures. *Europhys. Lett.* **61**, 375–381 (2003).

[33] Pennec, Y. *et al.* Supramolecular gratings for tuneable confinement of electrons on metal surfaces. *Nature Nanotech.* **2**, 99–103 (2007).

[34] Clair, S., Pons, S., Brune, H., Kern, K. & Barth, J. V. Mesoscopic metallosupramolecular texturing by hierarchic assembly. *Angew. Chem. Int. Ed.* **44**, 7294–7297 (2005).

[35] Bürgi, L., Knorr, N., Brune, H., Schneider, M.A. & Kern, K. Two-dimensional electron gas at noble-metal surfaces *Appl. Phys. A* **75**, 141–145 (2002).

[36] Crain, J. N., Stiles, M. D., Stroscio, J. A., & Pierce, D. T. Electronic Effects in the Length Distribution of Atom Chains *Phys. Rev. Lett.* **96**, 156801 (2006).

FIGURE CAPTIONS

FIG. 1: Homogenous electronic properties of gold vicinal surfaces.

a, STM image of the topography of a clean Au(788) surface. Dashed lines indicate a unit cell of the reconstruction periodicity including a hcp (left) and a fcc (right) domain. The domains are separated by stacking fault lines. **b**, **c**, **d**, Corresponding dI/dV images ($30 \times 10 \text{ nm}^2$) recorded in open feedback loop -0.41 V , -0.37 V and -0.065 V respectively. The confinement by the step edges induces quantum well states. The confinement leads to a modification of the band structure of the Shockley state and a specific modulation of the local electronic properties. In particular, the onset energy of the surface band is shifted and the LDOS is modulated perpendicular to the step edges. The LDOS patterns remain homogenous over large distances, and also depend on the energy. At low energy, **b**, the electronic density is centred in the middle of the terraces because only the fundamental eigenstate in the perpendicular direction is excited at this energy. The LDOS is also modulated along the terraces, with the maxima first localised in hcp domains. As the energy increases, **c**, the maxima shift to the fcc domains because of the effect of the reconstruction-induced potential on the electronic properties[24]. Increasing the energy further, **d**, leads to features related to excited states in the perpendicular direction and a smearing of the reconstruction effect in the parallel direction. Stabilisation parameters: $V=0.6 \text{ V}$, $I=0.75 \text{ nA}$. Red and yellow correspond to high DOS.

FIG. 2: Periodic electronic patterns on self-organised superlattice of silver nanostructures on Au(788).

a, STM image ($70 \times 70 \text{ nm}^2$) of the surface topography recorded at 5K. The shapes of the islands and their spacing are very homogenous. The islands are connected to the step edges of gold. The nanostructures were grown at 130K. Their average size is 4.5 nm^2 . Stabilisation parameters: $V=-0.6 \text{ V}$, $I=0.4 \text{ nA}$. Coverage: 0.22 monolayer (ML). **b**, Normalised distribution of the distance between 2 consecutive Ag islands: $\text{HWHM}=0.13$. **c**, Normalised distribution of the lateral size of the triangular islands: $\text{HWHM}=0.15$. The distributions were evaluated by processing data corresponding to more than 1800 islands grown at 130K. **d**, and **e**, Typical dI/dV images ($70 \times 30 \text{ nm}^2$) recorded in closed feedback loop. The LDOS patterns remain homogenous over

large distances, and also depend on the energy. Stabilisation parameters: $V=-0.3V$ and $V=0.2V$ respectively, $I=0.4nA$. Red and yellow correspond to high DOS.

FIG. 3: Local view of Ag/Au nanostructures.

a, STM image ($12\times 9nm^2$) of the topography formed by the self-organised growth of the Ag/Au(788) system with 0.22ML of Ag. Stabilisation parameters: $V=0.8V$, $I=0.4nA$. **b, c, d, e**, Corresponding dI/dV images acquired in open feedback loop at $-0.41eV$, $-0.37eV$, $-0.25eV$ and $-0.065eV$ respectively. Stabilisation parameters: $V=0.4V$, $I=0.2nA$. **f**, Schematic view of a few unit cells of the periodic potential seen by the surface state electrons, with dark regions corresponding to repulsive potentials. Fcc domains are supposed to be slightly repulsive; Ag islands correspond to low potentials; and step edges are strongly repulsive. The effects of stacking fault lines on the electrons are small and are therefore disregarded.

FIG. 4: Electronic density for different growth parameters.

a, STM image ($17\times 17nm^2$) of the topography formed by the self-organised growth of the Cu/Au(23 23 21) system with 0.22ML of Cu. **b, c, d, and e**, Corresponding dI/dV images at $-0.46eV$, $-0.33eV$, $-0.12eV$ and $+0.3eV$. At low energy, **b**, one maximum per unit cell (corresponding to the fundamental state) can be seen. Increasing the energy, **c**, leads first to two LDOS maxima in the larger direction of the unit cell and then, **d**, to maxima in the shorter direction (perpendicular to the steps). This is in agreement with the simple view of a surface state in a rectangular box composed of the step edges and the regularly spaced strongly repulsive Cu islands. At $0.3eV$ above E_F , **e**, the first eigenstate of the Cu island induces an enhancement of the LDOS inside the nanostructures. Stabilisation parameters: $V=0.54V$, $I=0.4nA$. **f**, schematic view of the potential seen by the surface states. **g**, STS spectra at the centre of different self-organised nanostructures on Au(23 23 21). 1 and 2 correspond to triangular Ag islands for 0.34ML and 0.26ML, while 3 corresponds to the average spectrum of the Cu bilayer islands shown in **a**.

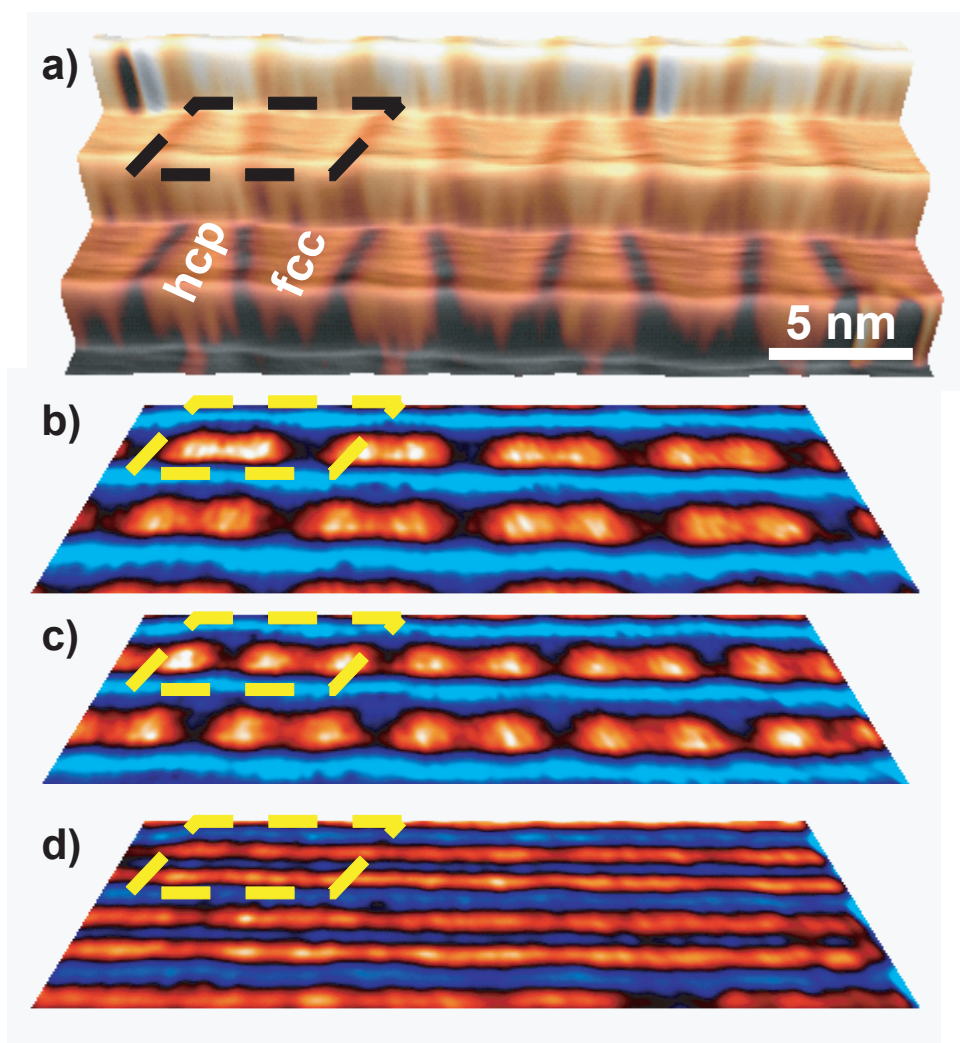


Figure 1

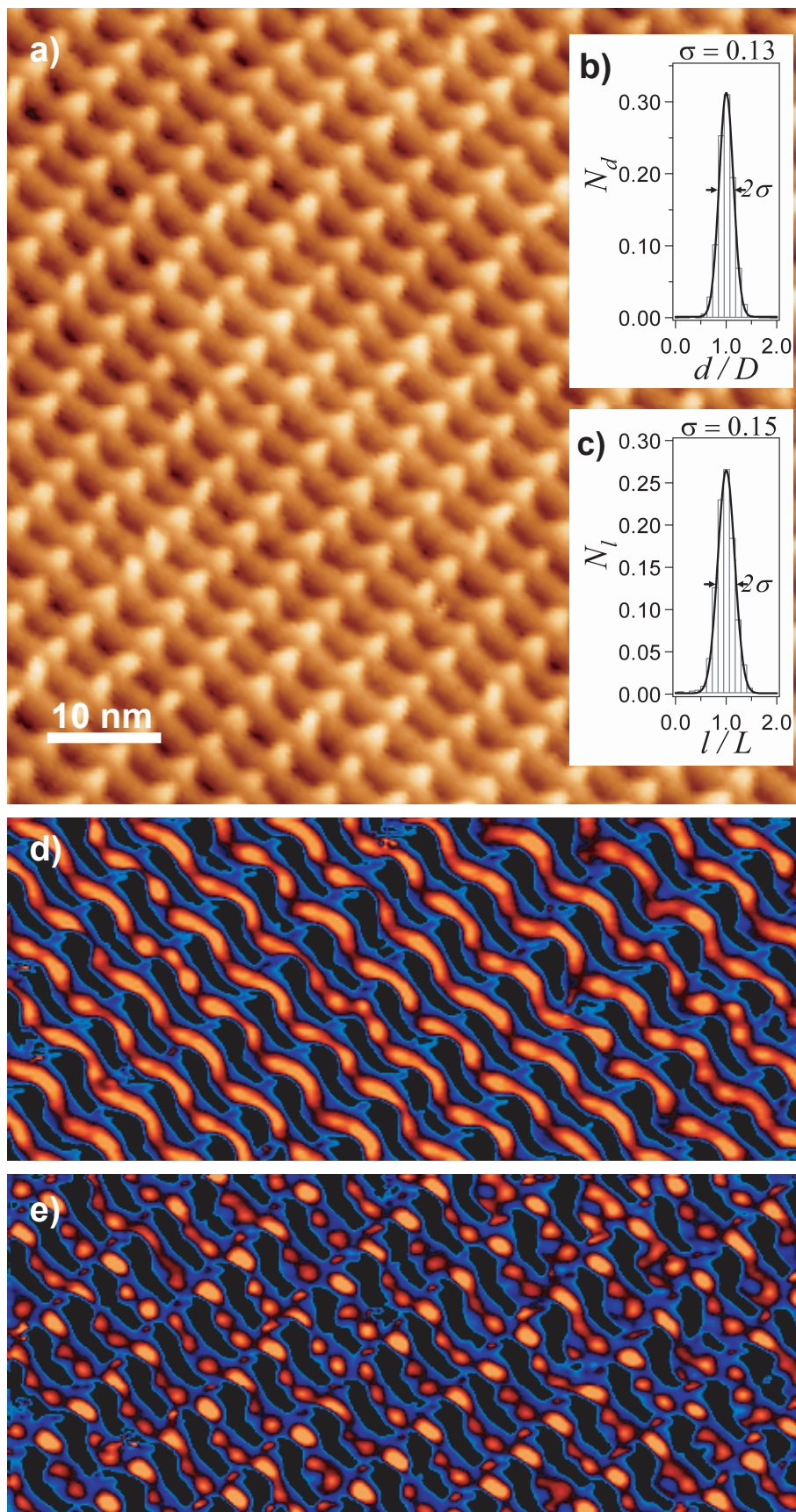


Figure 2

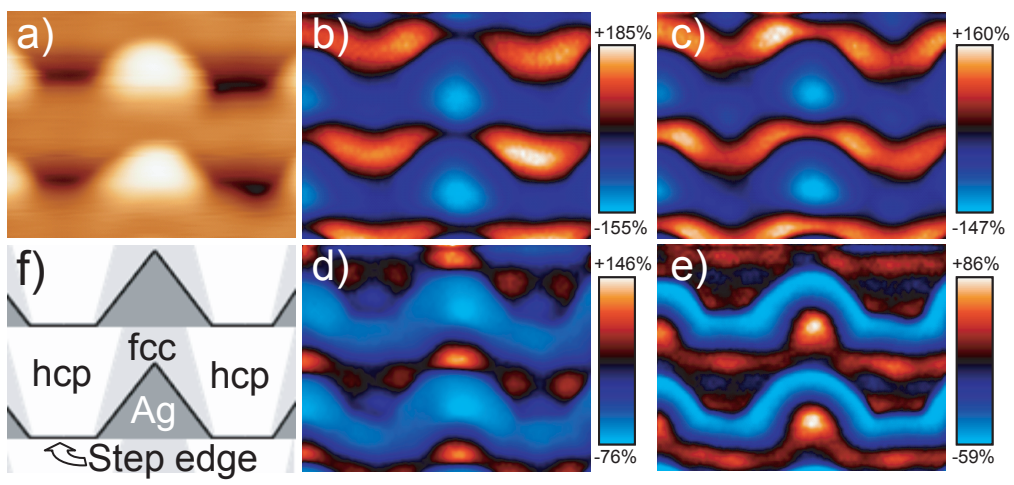


Figure 3

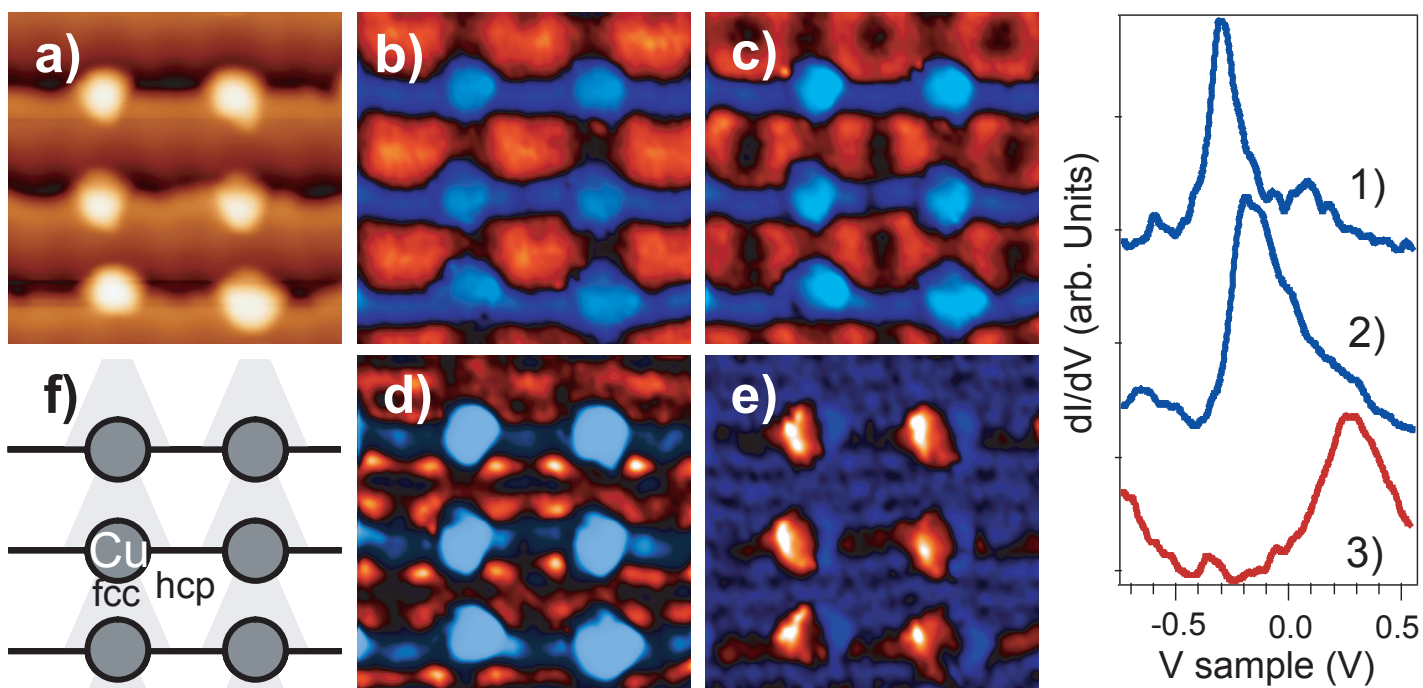


Figure 4